Antialiasing of Kirchhoff operators by reciprocal parameterization[a]

[a]Published in Journal of Seismic Exploration, v. 10, 293-310 (2002)

Sergey Fomel

ABSTRACT

I propose a method for antialiasing Kirchhoff operators, which switches between interpolation in time and interpolation in space depending on the operator dips. The method is a generalization of Hale's technique for dip moveout antialiasing. It is applicable to a wide variety of integral operators and compares favorably with the popular temporal filtering technique. Simple synthetic examples demonstrate the performance and applicability of the proposed method.

INTRODUCTION

Integral (Kirchhoff-type) operators are widely used in seismic imaging and data processing for such tasks as migration, dip moveout (Hale, 1991), azimuth moveout (Biondi et al., 1998), and shot continuation (Bagaini and Spagnolini, 1996). In theory, the operators correspond to continuous integrals. In practice, the integration is replaced by summation and becomes prone to sampling errors. A common problem with practical implementation of integral operators is the operator aliasing, caused by spatial undersampling of the summation path (Lumley et al., 1994). When the integration path is parameterized in the spatial coordinate, as it is commonly done in practice, the steeper part of the summation path becomes undersampled.

The operator aliasing problem, as opposed to the data aliasing and image aliasing problems, is discussed in detail by Lumley et al. (1994) and Biondi (2001). It arises when the slope of the operator traveltime exceeds the limit, defined by the time and space sampling of the data - the Nyquist frequencies (Claerbout, 1992a). Even if the input data are not aliased, operator aliasing can cause severe distortions in the output. Several successful techniques have been proposed in the literature to overcome the operator aliasing problem. Different versions of the temporal filtering method were suggested by Gray (1992) and Lumley et al. (1994) and further enhanced by Abma et al. (1999) and Biondi (2001). This method reduces the aliasing error by limiting the rate of change in the integrand (the input data) with temporal filtering. Unfortunately, this approach is suboptimal in the case of rapid changes in the summation path gradient. A different approach to antialiasing was suggested by Hale (1991) for the integral dip moveout. Hale's approach provides accurate results by parameterizing the operator in the time coordinate rather than the space coordinate. Unfortunately, this approach requires an additional expense of interpolation in both space and time coordinates for computing the flat part of the operator.

In this paper, I propose a new antialiasing method derived from the time-slice technique, developed by Hale (1991). The method switches between interpolation in time and interpolation in space depending on the local operator dips. It is particularly attractive for computing 3-D operators with rapidly varying dips and limited aperture (Fomel and Biondi, 1995). Synthetic examples show the superior performance of the new method in comparison the temporal filtering approach.

OVERVIEW OF EXISTING METHODS

I start with reviewing the existing approaches to operator antialiasing and discussing their main principles and limitations. The two reviewed approaches are temporal filtering, as suggested by Gray (1992) and Lumley et al. (1994), and Hale's spatial filtering technique, developed originally for an integral implementation of the dip moveout operator (Hale, 1991).

Temporal filtering

The temporal filtering idea follows from the well-known Nyquist sampling criterion. With application to integral operators, the Nyquist criterion takes the form

$$\Delta x \leq \frac{\Delta t}{|\partial t / \partial x|} \;, \tag{1}$$

where $t(x)$ is the traveltime of the operator impulse response, Δx is the space sampling interval and Δt is the time sampling interval. In the steep parts of the traveltime curve, the sampling criterion (1) is not satisfied, which causes aliasing artifacts in the output data. To overcome this problem, the method of local triangle filtering (Claerbout, 1992a; Lumley et al., 1994) suggests convolving the traces of the generated impulse response with a triangle-shaped filter of the length

$$\delta t = \Delta x \, |\partial t / \partial x| \;. \tag{2}$$

Cascading operators of causal and anticausal numerical integration is an efficient way to construct the desired filter shape.

Triangle filters approximate the ideal (sinc) low-pass time filters. The idea of using low-pass filtering for antialiasing (Gray, 1992) is illustrated in Figure 1. When a steeply dipping event is included in the operator, its counterpart in the frequency domain wraps around to produce the aliasing artifacts. Those are removed by a dip-dependent low-pass filtering.

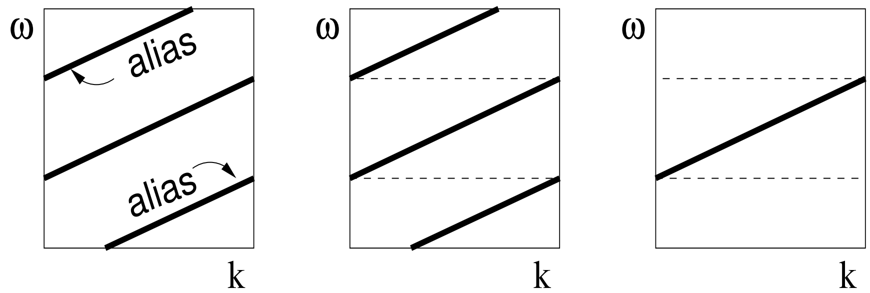

Figure 1: Schematic illustration of low-pass antialiasing (triangle filters). The aliased events are removed by low-pass filtration on the temporal frequency axis. The width of the low-pass filter depends on dips of the aliased events.

The method of low-pass filtering is less evident in the case of a three-dimensional integral operator. We can take the length of a triangle filter proportional to the absolute value of the time gradient (Lumley et al., 1994), the maximum of the gradient components in the two directions of the operator space (Abma et al., 1999), or the sum of these components. The latter follows from considering the 3-D operator as a double integration in space. Decoupling the 3-D integral into a cascade of two 2-D operators suggests convolving two triangle filters designed with respect to two coordinates of the operator. In this case, the length of the resultant filter is approximately equal to

$$\delta t = \Delta x \left|\partial t / \partial x\right| + \Delta y \left|\partial t / \partial y\right| \,, \tag{3}$$

and its shape is smoother than that of a triangle filter (Figure 2).

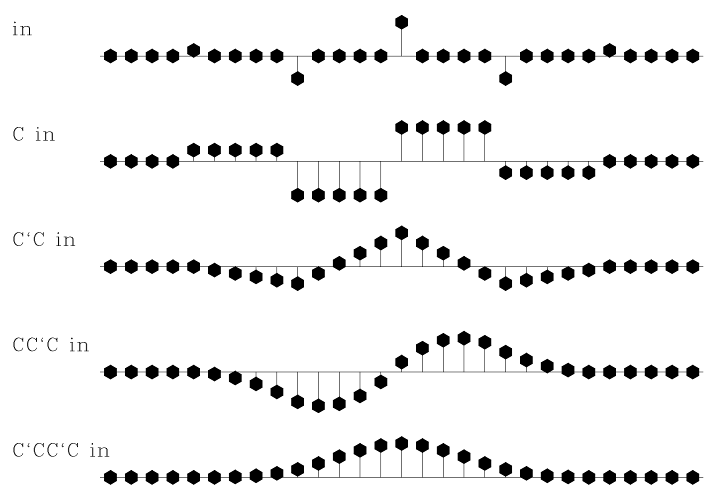

Figure 2: Building the smoothed filter for 3-D antialiasing by successive integration of a five-point wavelet. C denotes the operator of causal integration, C' denotes its adjoint (the anticausal integration). The result is equivalent to the convolution of two equal triangle filters.

The temporal filtering method was proven to be an efficient tool in the design of stacking operators of different types. However, when the operator introduces rapid changes in the length and direction of the traveltime gradient, it leads to an inexact estimation of the filter cutoff (triangle length for the method of triangle filtering) at the curved parts of the operator. Consequently, the high-frequency part of the output can be distorted, causing a loss in the image resolution.

Hale's method

Considering the case of integral dip moveout, Hale (1991) points out that the steep parts of the operator, while aliased in the space (midpoint) coordinate, are not aliased with respect to the time coordinate. He suggests replacing the conventional $t(x)$ parameterization of the DMO impulse response by $x(t)$ parameterization. Conventionally, the integral operators are implemented by shifting the input traces in space and transforming them in time. According to Hale's method, the traces are shifted in time and transformed along the $x(t)$ trajectories in space. Interpolation in time, required in the conventional approach, is replaced by interpolation in space. The idea of Hale's method is related to the idea of the "pixel-precise velocity transform" (Claerbout, 1992b).

The steep parts of the operator satisfy the criterion

$$\Delta t \leq \frac{\Delta x}{|\partial x / \partial t|} \; , \tag{4}$$

which is the the obvious reverse of inequality (1). Therefore, they are not aliased if defined on the time grid. In these parts, one can implement the operator by constant time shifts equal to the time sampling interval Δt. In the parts where the criterion (4) is not valid (the flat part of the DMO operator), Hale suggests reducing the length of the time shifts according to equality (2), where δt becomes less than Δt. He formulates the following principle of operator antialiasing:

> To eliminate spatial aliasing, simply never allow successive time shifts applied to the input trace to differ by more than one time sampling interval. Further restrict the difference between time shifts so that the spacing between the corresponding output trajectories never exceeds the CMP sampling interval.

The idea of Hale's method is illustrated in Figure 3. Increasing the density of spatial sampling by small successive time shifts implies increasing the Nyquist boundaries of the spatial wavenumber. Further interpolation is a low-pass spatial filtering that removes the parts of the spectrum beyond the Nyquist frequency of the output. If the dip of the operator does not vary between neighboring traces (the operator is a straight line as in the slant stack case), Hale's approach will produce essentially the same result as that of temporal filtering. Triangle filters in this case approximately correspond to linear interpolation in space between adjacent traces (Nichols, 1993). The difference between the two approaches occurs if the local dip varies in space as in the case of a curved operator, such as DMO. In this case, Hale's approach provides a more accurate space interpolation of the operator and preserves the high-frequency part of its spectrum from distortion.

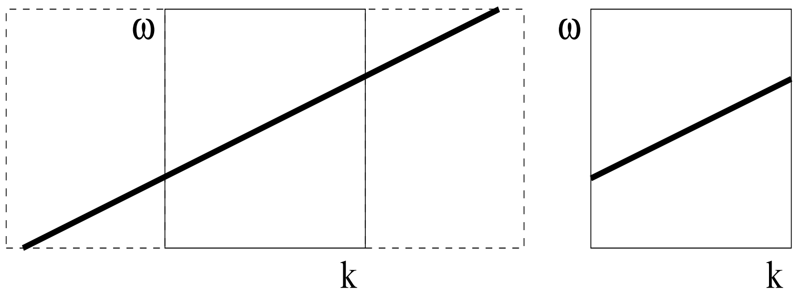

Figure 3: Schematic illustration of Hale's antialiasing. The aliased events are removed by spatial interpolation. In the frequency domain, the interpolation consists of widening and low-passing on the wavenumber axis. The low-pass spatial filtering does not depend on dip.

Hale's method has proven to preserve the amplitude of flat reflectors from aliasing distortions, which is the simplest antialiasing test on a DMO operator. The most valuable advantage of this method in the fact that the implied low-pass spatial filtering (interpolation) does not depend on the operator dip and is controlled by the Nyquist boundary of the spectrum only (compare Figures 1 and 3). This is especially important, when the local dip of the operator changes rapidly and therefore cannot be estimated precisely by finite-difference approximation at spatially separated traces. Such a situation is common in dip moveout and azimuth moveout integral operators, as well as in prestack Kirchhoff migration.

A weakness of the method is the necessity to switch from interpolation in space to two-dimensional interpolation in both the time and the space variables, when trying to construct the flat part of the operator. In the next section, I show how to avoid the expense of the additional time interpolation required by Hale's method of antialiasing.

PROPOSED TECHNIQUE

We can use the reciprocity of the time parameterization and the space parameterization of integral operators, discovered by Hale, to arrive at the following antialiasing technique.

For simplicity, let us consider the two-dimensional case first. The linearity of a two-dimensional integral operator allows us to decompose this operator into two parts. The first part corresponds to the steep part of the travel-time function, which satisfies the time-sampling criterion (4). The second term corresponds to the flat part of the traveltime, which satisfies the space-sampling criterion (1). The first part is not aliased with respect to the time sampling interval, while the second one is not aliased with respect to the space sampling. We can apply interpolation in time to construct the flat part. Reciprocally, interpolation in space is applied to construct the steep part of the operator in the fashion of Hale's time-shifting method. The amplitude difference between the two integrals is simply the Jacobian term

$$\frac{\text{amp}_t}{\text{amp}_x} = \left|\frac{\partial x}{\partial t}\right| \frac{\Delta t}{\Delta x} = \frac{\Delta t}{\delta t} \leq 1 \; . \tag{5}$$

According to the proposed modification, Hale's antialiasing principle is reformulated, as follows:

In the steep part of an integral operator, never allow successive time shifts applied to the input trace to differ by more than one time sampling interval. In the flat part of the operator, never allow successive space shifts to differ by more than one space sampling interval.

Figure 4, borrowed from Claerbout (1995), illustrates the basic idea of the proposed technique. It clearly shows the difference between the flat and steep parts of migration hyperbolas. To observe the reciprocity, rotate the figure by 90 degrees.

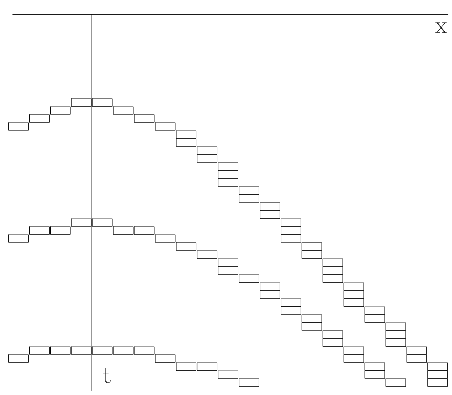

Figure 4: Figure borrowed from Claerbout (1995) to illustrate the reciprocity antialiasing. The flat parts of the hyperbolas require interpolation in time. The steep parts of the hyperbolas require interpolation in space.

To compare the proposed antialiasing method with the temporal filtering method, I test the antialiased migration program on simple 2-D synthetic tests. Figure 5 shows a simple model and the modeling results from modeling without antialiasing, with temporal filtering, and with the proposed reciprocity method. The modeling results were migrated with the corresponding migration operators to obtain the image of the model in Figure 6. Both the temporal filtering and the proposed method succeed in removing the major aliasing artifacts. However, the reciprocity method demonstrates a higher resolution and a better preservation of the frequency content.

These properties are examined more closely in the next synthetic example. Figure 7 shows a more sophisticated synthetic model that contains a fault, an unconformity

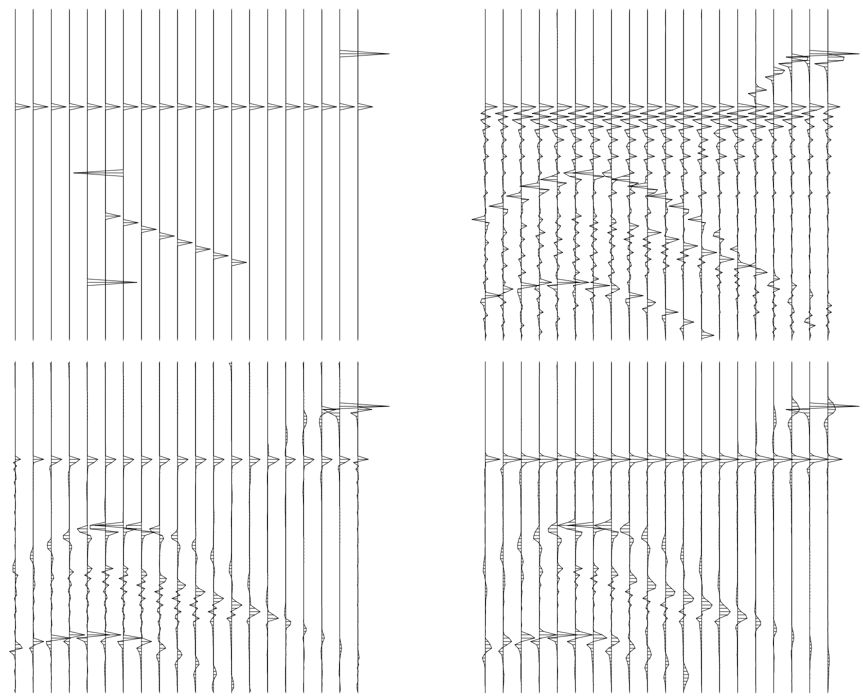

Figure 5: Top left is a synthetic model. Top right is modeling without antialiasing. Bottom left is modeling with reciprocity antialiasing (the proposed method). Bottom right is modeling with antialiasing by temporal filtering.

and layered structures (Claerbout, 1995). For better displaying, I extract the central part of the model and compare it with the migration results of different methods in Figure 8. Comparing the plots shows that the reciprocity method successfully removes the aliasing artifacts (round-off errors) of the aliased (nearest neighbor interpolation) migration. At the same time, it is less harmful to the high-frequency components of the data than triangle filtering. This conclusion finds an additional support in Figure 9 that displays the average spectrum of the image traces for different methods. Both of the antialiasing methods remove the high-frequency artifacts of the nearest neighbor modeling and migration. The reciprocity method performs it in a gentler way, preserving the high-frequency components of the model.

The algorithm sequence of the antialiased migration is illustrated in Figures 10 and 11. The two plots in Figure 10 show the steep-dip and flat-dip modeling respectively. The superposition of these two terms is the resultant antialiased data shown in the left plot of Figure 12. The right plot of Figure 12 shows the migrated image obtained by adding the flat-dip (left of Figure 11) and steep-dip (right of Figure 11) migrations.

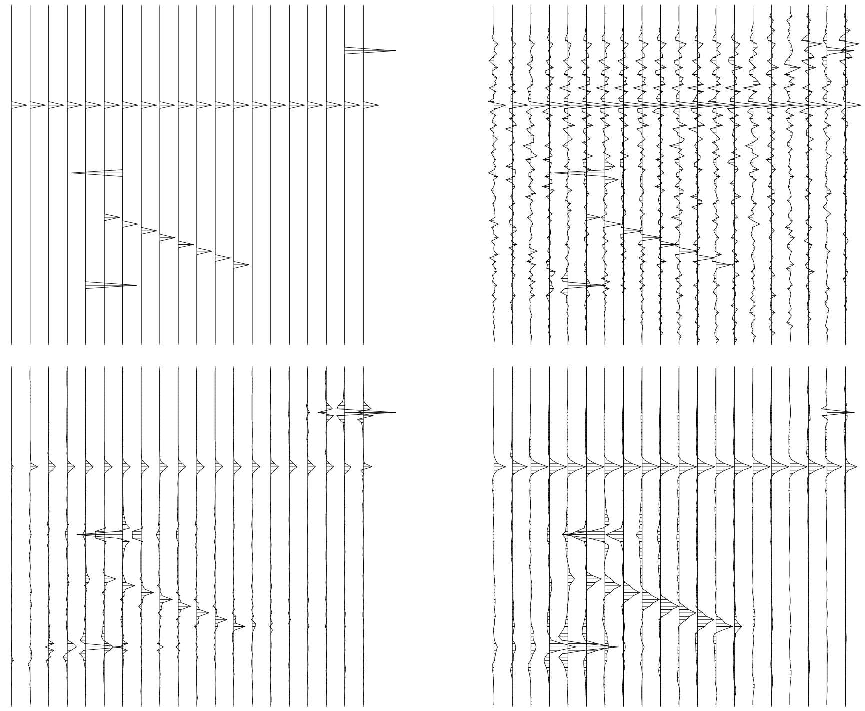

Figure 6: Top left plot is the synthetic model. The other plots are migrations of the corresponding data shown in the previous figure . Top right is a migration without antialiasing. Bottom left is a migration with reciprocity antialiasing (the proposed method). Bottom right is a migration with triangle filter antialiasing.

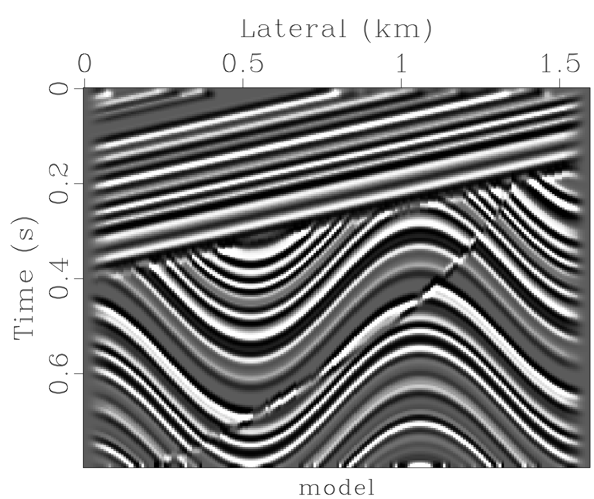

Figure 7: Synthetic model used to test the antialiased migration program.

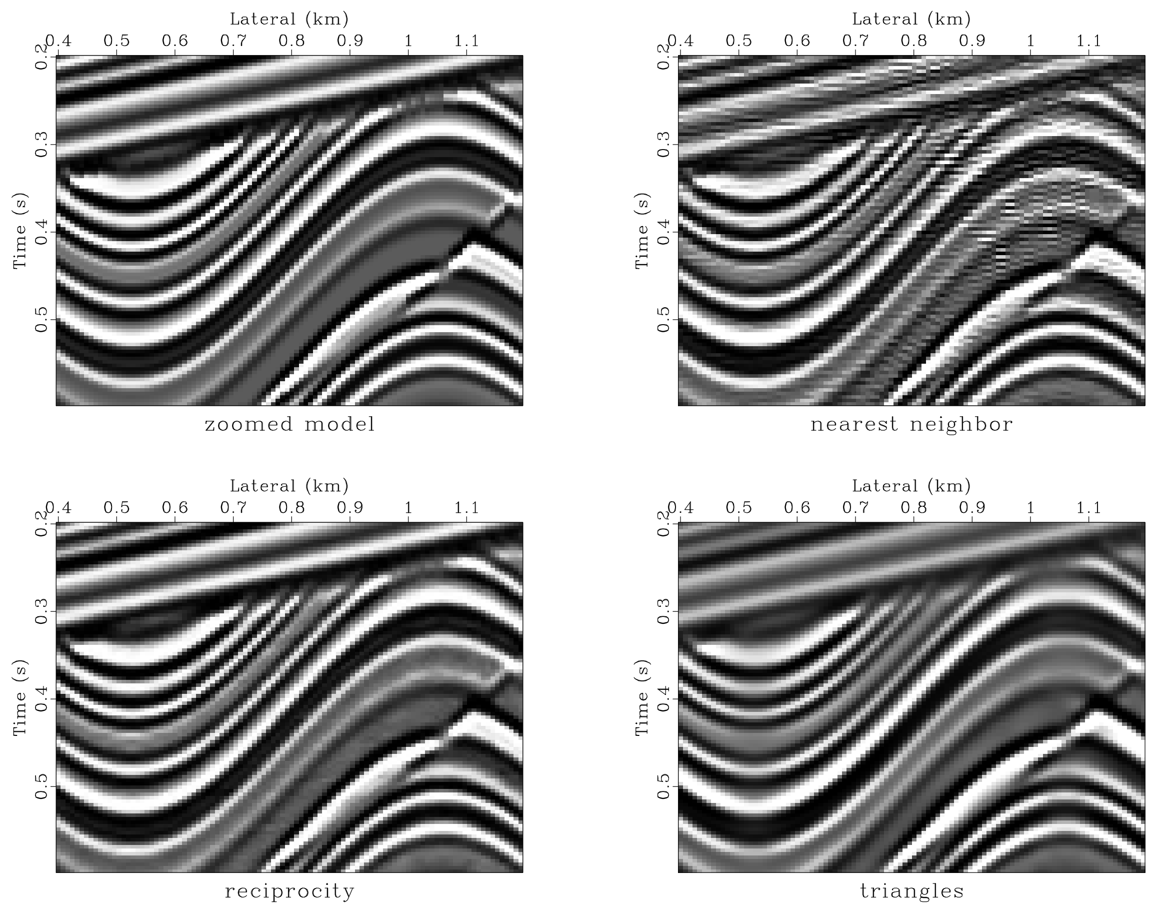

Figure 8: Top left plot is a zoomed portion of the synthetic model. The other plots are migrated images. Top right is a migration without antialiasing. Bottom left is a migration with reciprocity antialiasing (the proposed method). Bottom right is a migration with triangle filter antialiasing.

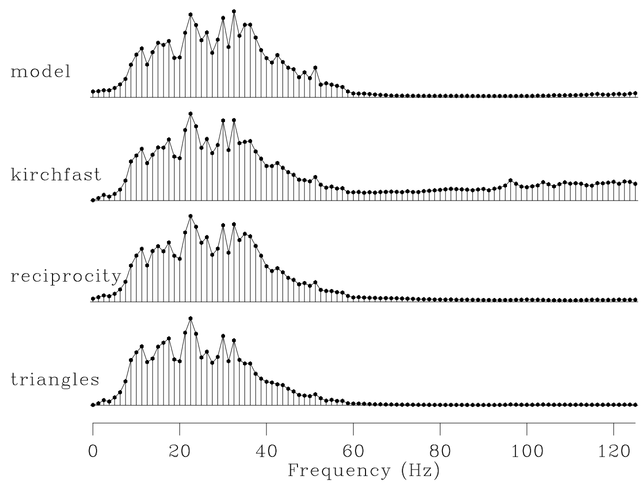

Figure 9: Top is the spectrum of the model. The other plots are the spectra of the migrated images. The second plot corresponds to the modeling/migration without account for antialiasing. The third plot is modeling/migration with the reciprocity antialiasing. The bottom plot is modeling/migration with triangle antialiasing.

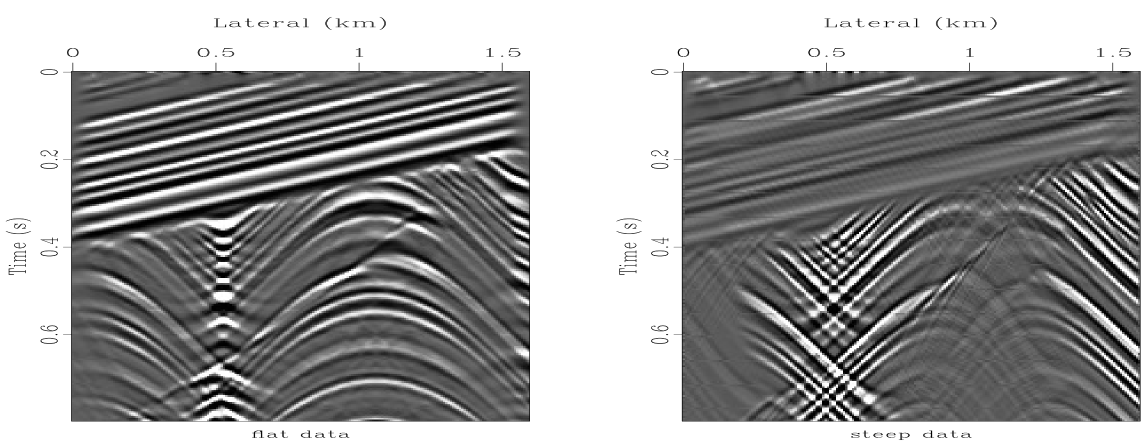

Figure 10: Antialiased modeling. Left corresponds to the flat-dip term. Right corresponds to the steep-dip term.

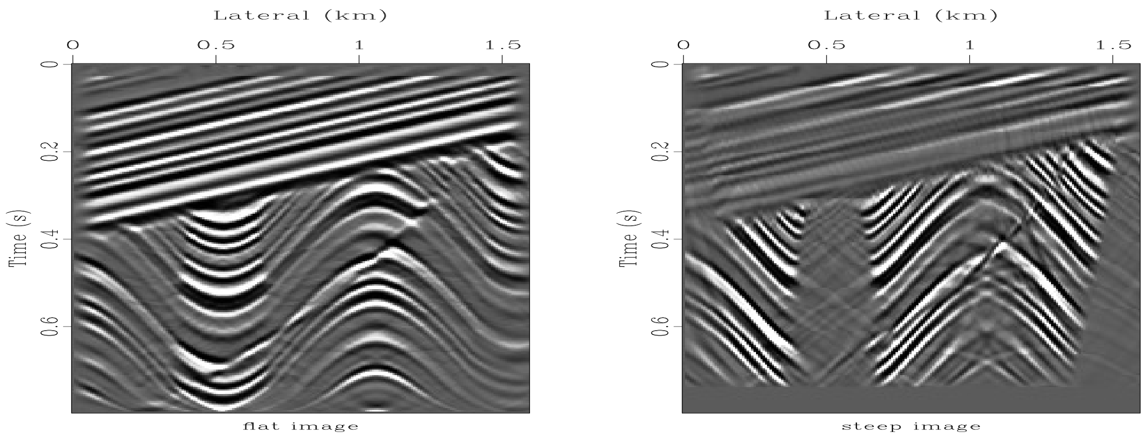

Figure 11: Antialiased migration. Left corresponds to the flat-dip term. Right corresponds to the steep-dip term.

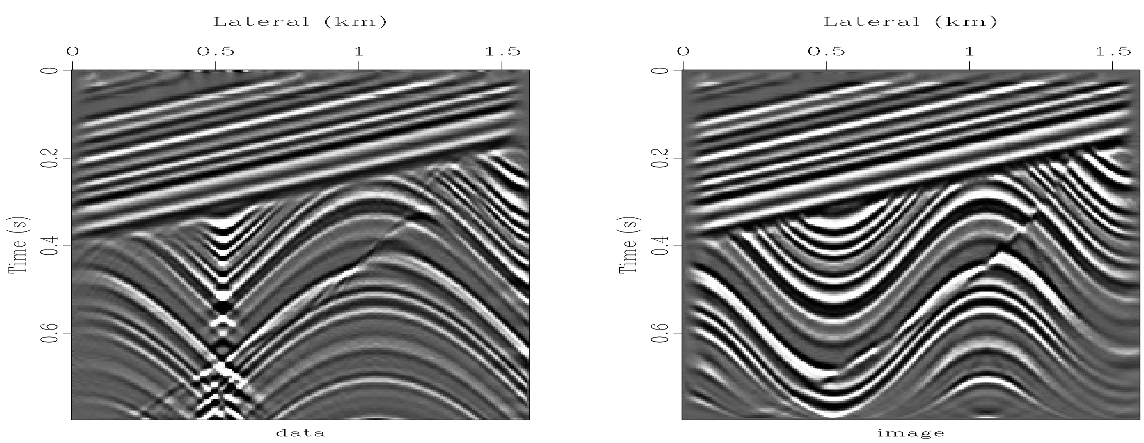

Figure 12: Antialiased modeling and migration. Left is the superposition of the flat-dip and steep-dip modeling. Right is superposition of the flat-dip and steep-dip migration.

3-D antialiasing

The proposed method of antialiasing is easily generalized to the case of a three-dimensional integral operator. In this case, we need to consider three different parameterizations: $t(x,y)$, $x(t,y)$, and $y(t,x)$ and switch from one of them to another according to the rule:

- if $\Delta t \geq \Delta x \, |\partial t/\partial x|$ and $\Delta t \geq \Delta y \, |\partial t/\partial y|$, use $t(x,y)$,
- if $\Delta x \geq \Delta t \, |\partial x/\partial t|$ and $\Delta x \geq \Delta y \, |\partial x/\partial y|$, use $x(t,y)$,
- if $\Delta y \geq \Delta t \, |\partial y/\partial t|$ and $\Delta y \geq \Delta x \, |\partial y/\partial x|$, use $y(t,x)$.

Following Biondi (2001), I illustrate 3-D antialiasing by applying prestack time migration on a single input trace. The results are shown in Figures 13, 14 and 15. The result without any antialiasing protection (Figure 13) contains clearly visible aliasing artifacts caused by the steeply dipping parts of the operator. Antialiasing by temporal filtering (Figure 14) removes the artifacts but also attenuates the steeply dipping events. Antialiasing by the proposed reciprocal parameterization (Figure 15) removes the aliasing artifacts while preserving the steeply dipping events and the image resolution.

CONCLUSIONS

I have introduced a new method of antialiasing integral operators, modified from Hale's approach to antialiased dip moveout. The method compares favorably with the popular temporal filtering technique. The main advantages are:

1. Accurate handling of variable operator dips.
2. Consequent preservation of the high-frequency part of the data spectrum, leading to a higher resolution.
3. Easy control of operator amplitudes.
4. Easy generalization to 3-D.

The method possesses a sufficient numerical efficiency in practical implementations. Its most appropriate usage is for antialiasing operators with analytically computed summation paths, such as prestack time migration, dip moveout, azimuth moveout, and shot continuation.

ACKNOWLEDGMENTS

I thank Biondo Biondi for many helpful discussions. The financial support for this work was provided by the sponsors of the Stanford Exploration Project.

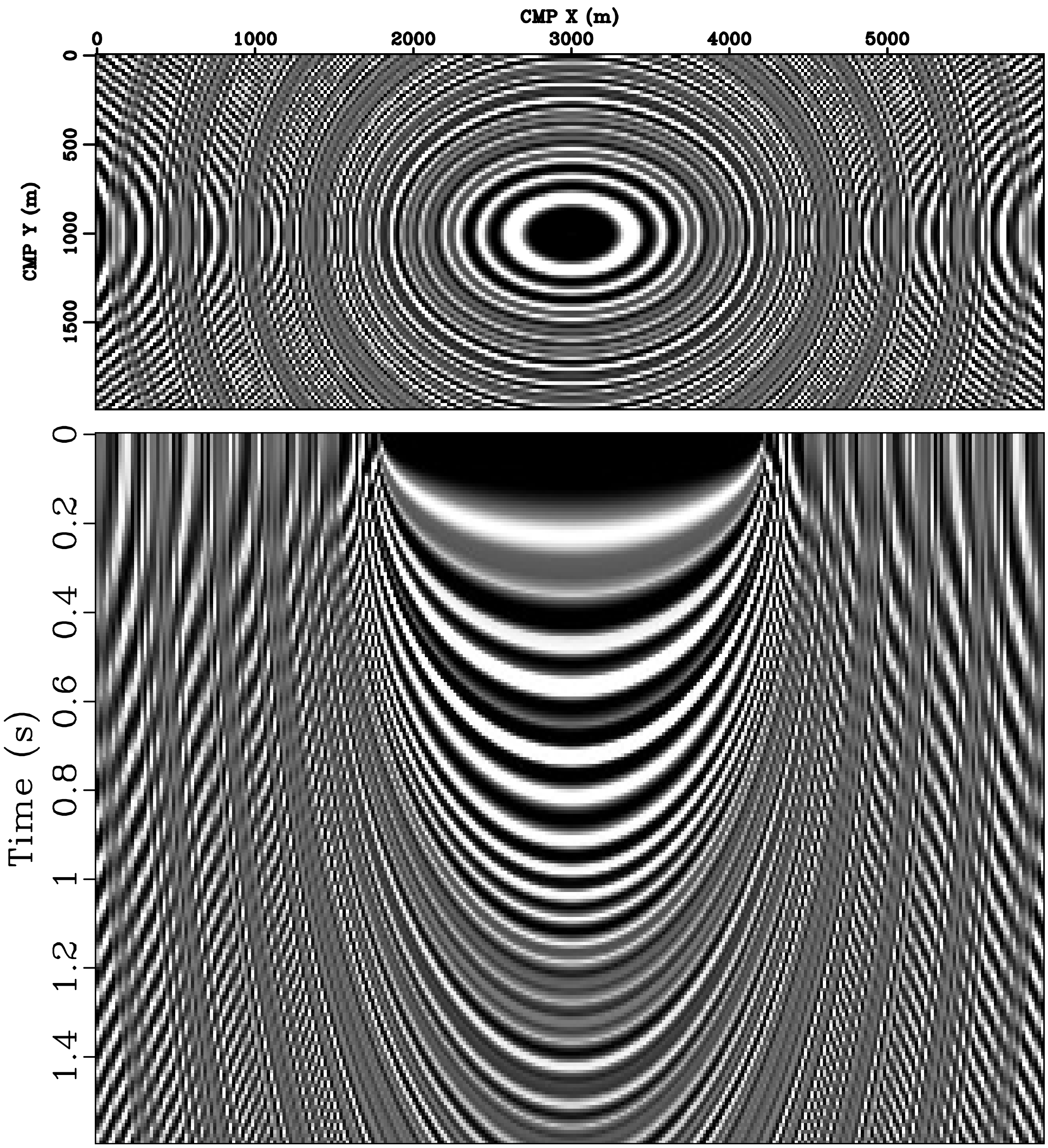

Figure 13: Prestack 3-D time migration of a single input trace. Top: time slice at 1 s. Bottom: vertical slice. No antialiasing protection has been applied. As a result, aliasing artifacts are clearly visible in the image.

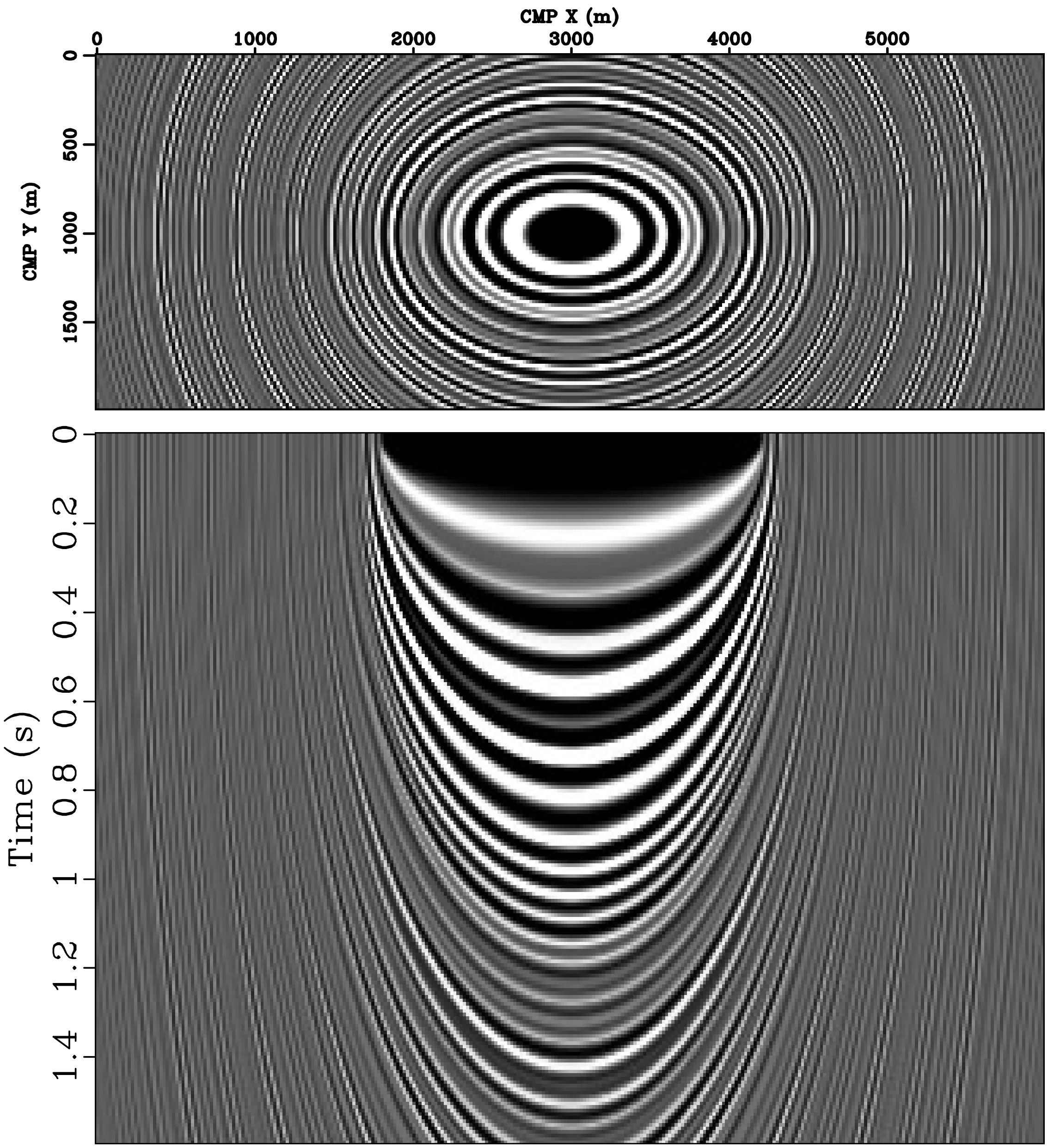

Figure 14: Prestack 3-D time migration of a single input trace. Top: time slice at 1 s. Bottom: vertical slice. Antialiasing by temporal filtering has been applied. Aliasing artifacts are removed, steeply dipping events are attenuated.

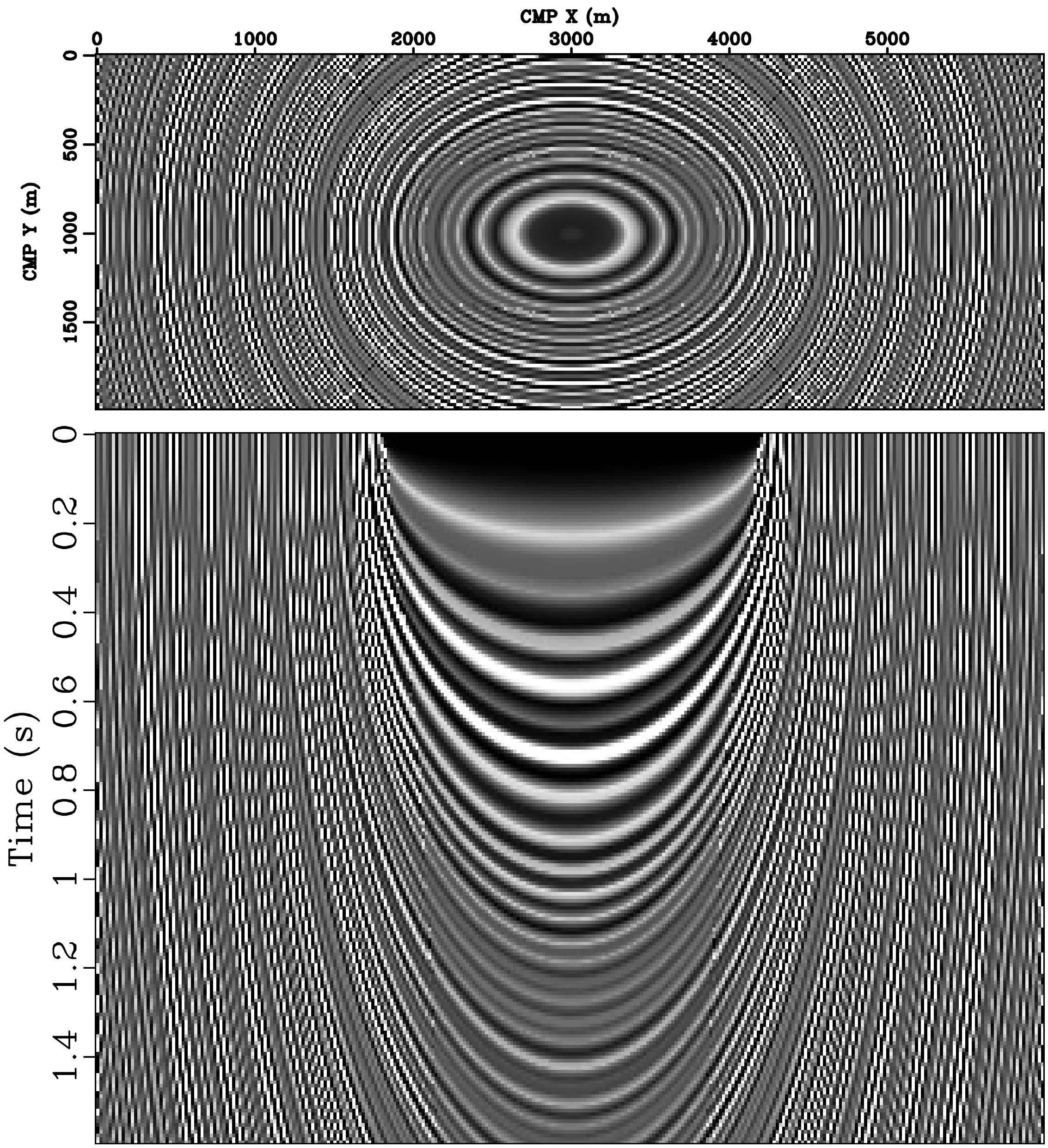

Figure 15: Prestack 3-D time migration of a single input trace. Top: time slice at 1 s. Bottom: vertical slice. The proposed reciprocal antialiasing has been applied. Aliasing artifacts are removed, steeply dipping events are preserved.

REFERENCES

Abma, R., J. Sun, and N. Bernitsas, 1999, Antialiasing methods in Kirchhoff migration: Geophysics, **64**, 1783–1792.

Bagaini, C., and U. Spagnolini, 1996, 2-D continuation operators and their applications: Geophysics, **61**, 1846–1858.

Biondi, B., 2001, Kirchhoff imaging beyond aliasing: Geophysics, **66**, 654–666.

Biondi, B., S. Fomel, and N. Chemingui, 1998, Azimuth moveout for 3-D prestack imaging: Geophysics, **63**, 574–588.

Claerbout, J. F., 1992a, Anti aliasing, *in* SEP-73: Stanford Exploration Project, 371–390.

———, 1992b, Earth Soundings Analysis: Processing Versus Inversion: Blackwell Scientific Publications.

———, 1995, Basic Earth Imaging: Stanford Exploration Project.

Fomel, S., and B. L. Biondi, 1995, Azimuth moveout: The operator parameterization and antialiasing, *in* SEP-89: Stanford Exploration Project, 89–108.

Gray, S. H., 1992, Frequency-selective design of the Kirchhoff migration operator: Geophys. Prosp., **40**, 565–572.

Hale, D., 1991, A nonaliased integral method for dip moveout: Geophysics, **56**, 795–805.

Lumley, D. E., J. F. Claerbout, and D. Bevc, 1994, Anti-aliased Kirchhoff 3-D migration: 64th Ann. Internat. Mtg, Soc. of Expl. Geophys., 1282–1285.

Nichols, D., 1993, Integration along a line in a sampled space, *in* SEP-77: Stanford Exploration Project, 283–294.